



The thermal degradation of polystyrene nanocomposite

Bok Nam Jang, Charles A. Wilkie*

Department of Chemistry Marquette University P.O. Box 1881, Milwaukee, WI 53201, USA

Received 12 November 2004; received in revised form 14 January 2005; accepted 18 January 2005

Available online 8 March 2005

Abstract

Nanocomposite formation brings about an enhancement of many properties for a polymer, including enhanced fire retardancy. This study was carried out to determine if the presence of clay causes changes in the degradation pathway of polystyrene. In the case of virgin PS, the degradation pathway is chain scission followed by β -scission (depolymerization), producing styrene monomer, dimer and trimer, through an intra-chain reaction. As the clay loading is increased, the evolved products produced through inter-chain reactions become significant. Due to the barrier effect of the clay layers, the radicals have more opportunity to undergo radical transfer, producing tertiary radicals, and then radical recombination reactions, producing head-to-head structures, and hydrogen abstraction from the condensed phase also occurs. In the presence of clay, the color of solid residues darkens as the clay content increases. It is thought that this color change is caused by the formation of conjugated double bonds in the presence of clay.

© 2005 Elsevier Ltd. All rights reserved.

Keywords: Polystyrene; Nanocomposites; Degradation

1. Introduction

Polymer–clay nanocomposites are one of the important modern technologies because of the capability of generating new polymer properties and, therefore, nanocomposites have attracted considerable attention. It is known that the addition of very small amounts clay (≤ 5 wt%) brings about a large enhancement of the mechanical properties [1,2], thermal and fire properties of the polymer [3,4]. Polystyrene (PS) nanocomposites are an area of active research, particularly since the reduction in the peak heat release rate, PHRR, is very large, typically about a 60% reduction is observed for well-dispersed clays in polystyrene [5,6].

There have been two mechanisms suggested for the reduction in PHRR, barrier formation [7] and paramagnetic radical trapping [8]. The formation of a barrier would inhibit mass transfer of degrading polymer to the vapor phase and it would also serve to insulate the underlying polymer from the radiation and both of these

would serve to reduce the peak heat release rate. X-ray photoelectron spectroscopy (XPS) measurements have been carried out [9–12] on polymer–clay nanocomposites and these have shown the clay does accumulate at the surface as the polymer degrades. The second pathway for reduction in PHRR, radical trapping, appears to only be important when the clay loading is quite low and the amount is insufficient to produce a good barrier. At the normal clay loading of 3–5%, the barrier formation is the accepted mechanism for the reduction in the peak heat release rate.

In this laboratory, TGA/FTIR was used to study the degradation of polystyrene nanocomposite and some changes were found in the wave number region between 1600–1630 cm^{-1} [13]. It was proposed that the degradation pathway of polymers was modified by the presence of clay in polymer–clay nanocomposites. However, there was no clear elucidation of the changes that occurred.

The thermal degradation pathway of virgin polystyrene has been well studied [14–21]. In this study, the possibility that the presence of the clay causes some chemical changes in the degradation pathway of polystyrene nanocomposites was explored, using TGA/FTIR for the thermal degradation and in-situ characterization of the evolved products and also collection of the evolved products for identification by GC/MS and FTIR.

* Corresponding author.

E-mail address: charles.wilkie@marquette.edu (C.A. Wilkie).

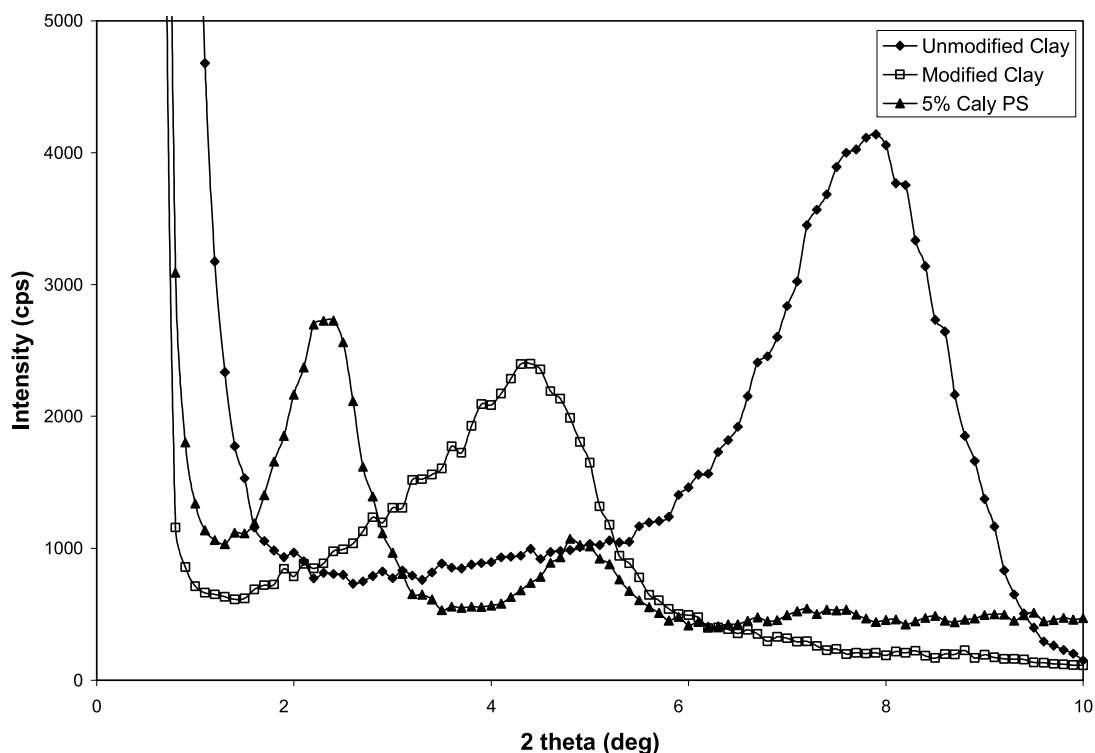


Fig. 1. XRD patterns for the hectorite clay, organically modified clay and 5% clay polystyrene nanocomposite.

2. Experimental

2.1. Modification of clay

Hectorite clay, supplied by Elementis Specialties, and Montmorillonite clay, supplied by Southern Clay Products, were modified by cationic exchange method using dimethylbenzyl hydrogenated tallow chloride (10A salt, supplied by Akzo-Nobel). A 10% mole excess of this salt was added to the clay slurry for the cationic exchange reaction in water, based on the cation exchange capacity of the clay. After stirring overnight, the modified clay was collected by filtration, washed thoroughly until no chloride was detected using aqueous silver nitrate and then dried in a vacuum oven at room temperature.

2.2. Preparation of nanocomposite

A bulk polymerization technique was utilized for the preparation of PS nanocomposite with varying clay content, using benzoyl peroxide as an initiator at 70 °C for 24 h. The residual monomer was removed in a vacuum oven at 80 °C; the procedure has been completely described in the literature [22].

2.3. Characterization of nanocomposite

Cone calorimetry and X-ray diffraction (XRD) were used to characterize the formation of nanocomposite. Cone

calorimetry was performed on an Atlas CONE2 according to ASTM E 1354-92 at an incident flux of 35 kW/m² using a cone shaped heater. Exhaust flow rate was 24 l/s and the electric spark was continuous until the sample ignited. The specimens for cone calorimetry were prepared by the compression molding of the sample (about 30 g) into 3 × 100 × 100 mm dimension square plaques. Typical results from cone calorimetry are reproducible to within ± 10%. XRD patterns were obtained using a Rigaku Geiger Flex, 2-circle powder diffractometer equipped with Cu-K α generator ($\lambda = 1.5404 \text{ \AA}$); generator tension was 50 kV and the current was 20 mA.

2.4. TGA/FTIR analysis and sampling of evolved products

TGA/FTIR was carried out in nitrogen at a heating rate of 20 °C/min and a nitrogen flow of 60 ml/min on Cahn TG 131 instrument that was connected to Mattson Research grade FTIR through stainless steel tubing. This instrument uses a sniffer tube that extends into the sample cup to remove the evolved gases; this sniffer tube removes gas at a rate of 40 ml/min. The evolved volatile products are introduced to the IR chamber through the tubing and analyzed by in-situ vapor phase FTIR. The temperature reproducibility of TGA is ± 3 °C and the fraction of non-volatile is ± 3%. The sample size was 40–60 mg. The evolved products during thermal degradation of each sample were collected using a cold trap at a temperature of –78 °C for the further analysis.

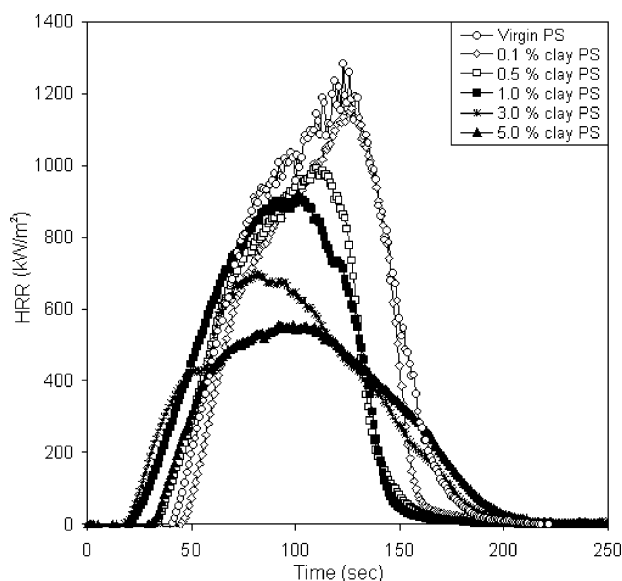


Fig. 2. Cone calorimetry results of polystyrene and polystyrene nanocomposites as a function of clay content.

2.5. Analysis of evolved condensable products

The collected evolved products in the trap were washed with acetonitrile. GC/MS spectra were obtained using an Agilent 6850 series GC connected to an Agilent 5973 Series MS (70 eV ionization energy) with temperature programming from 40 to 250 °C. The identities of evolved compounds were established by co-injection with authentic compounds and/or by the analysis of mass fragmentation pattern.

2.6. Analysis of solid residue sample

The solid residues after 40% mass loss were collected. A viscosity measurement for the soluble fraction of residue

was performed using Ubbelodeh viscometer at the concentration of 0.100 g/10.0 ml with toluene as a solvent at 25.0 °C. FTIR data were obtained for the solid residues after making KBr pellets using a Nicolet Magna Model 560 spectrometer. GC/MS data were also obtained after separating the low molecular compounds by extraction using toluene as a solvent and methanol as a non-solvent.

3. Results and discussion

3.1. The characterization of nanocomposite and TGA results

The formation of the nanocomposite of polystyrene and clay (the same results have been obtained with both hectorite and montmorillonite so the generic term clay is used herein to refer to both) was confirmed by XRD and cone calorimetry. Through the XRD study, it can be seen that the d-spacing of clay layer increases from 1.1 nm for the pristine clay to 2.1 nm in the case of organically modified clay and then finally to 3.8 nm for the bulk polymerized sample, as shown in Fig. 1; this implies that the polystyrene nanocomposite has an intercalated morphology. There has been previous work on this nanocomposite and the XRD that is reported herein agrees very well with that seen in the previous work [22]. In addition, TEM data has also been previously reported on similar systems and this confirms the intercalated nature of the nanocomposite [23].

Fig. 2 displays the heat release rate curves from cone calorimetry for each sample as a function of clay content; this shows the typical behavior of nanocomposites. As the clay content increases, the peak heat release rate (PHRR) decreases. In the case of 5% PS nanocomposite, the PHRR was reduced by 55% compared to virgin polystyrene, suggesting good nano-dispersion of clay in the polystyrene matrix. Previous work from this, and other, laboratories has shown that there is essentially no reduction in PHRR for a

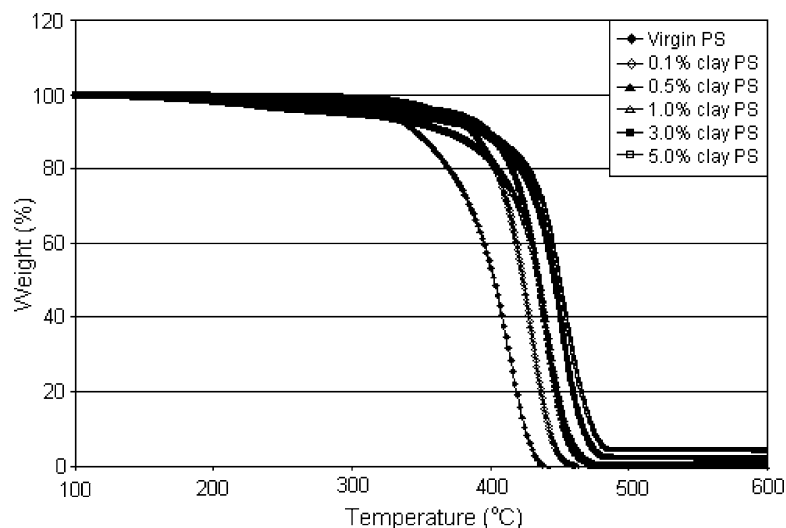


Fig. 3. TGA results of polystyrene and polystyrene nanocomposites.

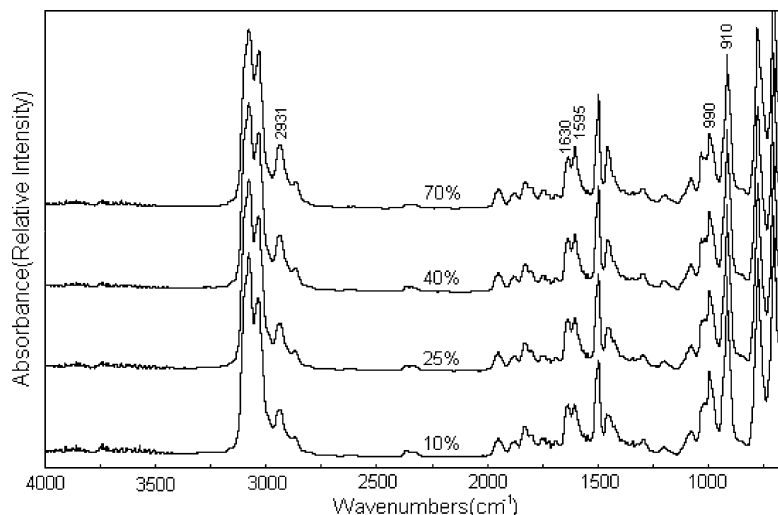


Fig. 4. In-situ vapor phase FTIR spectra of virgin polystyrene at various mass loss.

microcomposite while there is a good reduction for any system which shows good nano-dispersion [24,25].

The TGA curves of PS nanocomposites are shown in Fig. 3. Compared to virgin polystyrene, the thermal stability of the nanocomposite is always higher and it appears to increase as the clay content increases, at least up to 3% of clay. For instance, the temperature at 50% mass loss of 5% clay PS nanocomposite is about 50 °C higher than that of virgin PS. It is apparent that the thermal stability of nanocomposite is increased because of the presence of well-dispersed clay in polystyrene.

3.2. The analysis of the evolved gas products

The evolved gas products are characterized using vapor phase FTIR as a function of mass loss for each sample. Fig. 4 shows the vapor phase FTIR spectra of virgin polystyrene as a function of mass loss. It appears that there

is no difference in the peak positions and their relative intensities, which means that the thermally degraded products are qualitatively the same from the beginning to the end stage of degradation. Through the assignment of significant bands in Fig. 4, such as strong sp^2 carbon–hydrogen stretching band above 3000 cm^{-1} and the double bond vibration at 1630 cm^{-1} , it can be stated that the main evolved products contain phenyl alkenyl unit.

On the other hand, the FTIR results for the polystyrene nanocomposites show some gradual changes with the clay content, as shown in Fig. 5. The intensity of the sp^3 carbon–hydrogen stretching vibration increases as the clay content increases, especially 2970 cm^{-1} , which is assigned as the $sp^3\beta$ carbon–hydrogen (α methyl) stretching. The carbon–carbon double bond stretching at 1630 cm^{-1} and the C–H out-of-plane deformations [26] at 990 and 910 cm^{-1} decrease with the clay content. Thus, through a comparison of the vapor phase FTIR of the nanocomposite and the

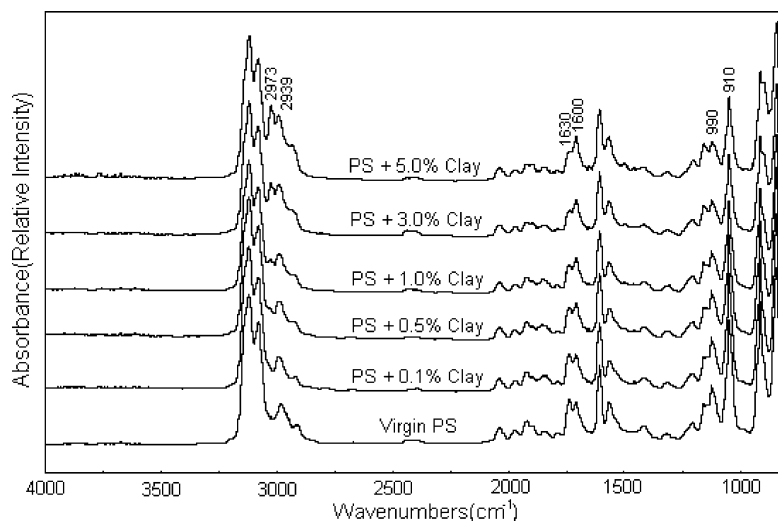


Fig. 5. In-situ vapor phase FTIR spectra of polystyrene and polystyrene nanocomposites at 50% mass loss.

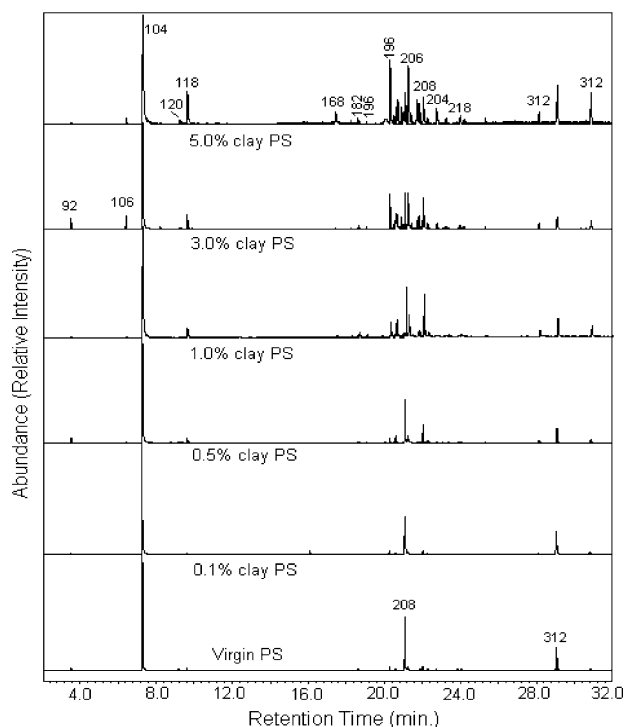


Fig. 6. GC traces for the evolved product of PS nanocomposites during thermal decomposition. The inset number denotes the m/z of the corresponding peak.

virgin polymer, it can be seen that some products having phenyl alkene unit have been lost, while some saturated structures appear.

In order to identify the structures of the evolved products, they were collected using a cold trap at $-78\text{ }^{\circ}\text{C}$ and GC/MS analysis was performed for the collected evolved products

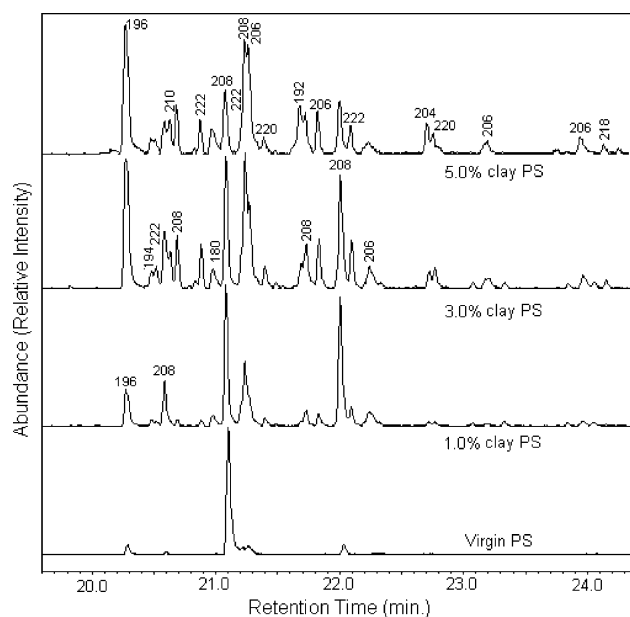


Fig. 7. Expanded GC traces for the two benzene ring region. The inset number denotes the m/z of the corresponding peak.

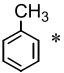
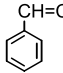
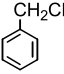
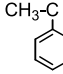
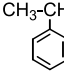
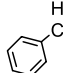
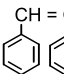
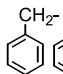
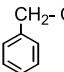
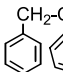
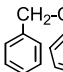
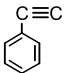
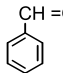
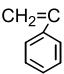
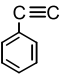
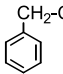
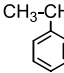
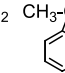
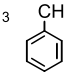
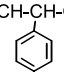
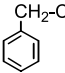
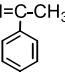
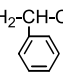
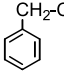
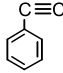
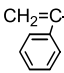
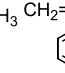
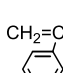
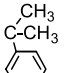
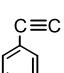
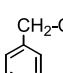
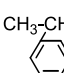
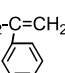

and the GC traces shown in Fig. 6. The structures were identified through the analysis of mass fragmentation pattern and/or by co-injection with authentic compounds. Table 1 exhibits the assigned structures for each peak in the GC traces. The evolved products can be classified into three groups; compounds having one benzene ring (retention time 3–14 min), two benzene rings (16–26 min) and three benzene rings (26–45 min). The evolved products having more than three benzene rings were not observed.

In the case of virgin polystyrene, three main peaks are observed, styrene monomer (m/z 104, 7.3 min), dimer (m/z 208, 21.1 min), and trimer (m/z 312, 29.2 min). As the clay content increases, the number of peaks increases and many additional structures may be assigned. Especially the two benzene ring region exhibits significant change, hence this region was expanded and it is shown in Fig. 7. In the two benzene ring region, the main evolved product of virgin polystyrene is styrene dimer (m/z 208, 21.1 min), while many additional structures are observed in the presence of clay and some head-to-head structures are assigned. These head-to-head structures are thought to be produced via radical recombination reactions. Considering the structures of m/z 208, 210, 222 etc. in Table 1, these compounds contain sp^3 β -carbon–hydrogen (α -methyl) which will give a strong stretching band at 2970 cm^{-1} , as already noted above.

The degradation pathway of virgin polystyrene proceeds by chain scission followed by depolymerization and the formation of the main evolved products, styrene monomer, dimer, and trimer, is shown in Scheme 1 [14–21]. After the formation of primary and secondary radicals via chain scission, the primary radical is transformed to the tertiary radical because of its increased stability, leading to the formation of α -methyl styrene via β -scission and the formation of another secondary radical. Hence, the secondary radical becomes the most abundant radical during the degradation and styrene, which is the most abundant evolved product, is produced via continuous β -scission (depolymerization). Since the secondary radical is also not stable, some of these may undergo radical transfer (hydrogen transfer) which produces the tertiary radical as shown in Scheme 1, and styrene dimer and trimer can be produced in a similar degradation fashion. The main evolved compounds during the degradation of virgin polystyrene contain carbon–carbon double bonds, which is supported by the strong band at 1630 cm^{-1} in the in-situ vapor phase FTIR results.

On the other hand, the GC traces of the polystyrene nanocomposites become complicated as the clay content of the nanocomposite increases. As clearly seen in Fig. 6, the relative abundance of styrene is decreased as the clay content increases, and, at the same time, new significant peaks, at m/z 's of 118 (9.6 min), 196 (20.4 min), 206 (21.3 min), 208 (21.2 min, 21.8 min), 222 (22.1 min) etc., are observed, which suggests that there are changes in degradation pathway in the presence of clay. Some

Table 1
The structures for the peaks in GC traces

<i>m/z</i>	Time(min)	Structures	<i>m/z</i>	Time(min)	Structures
92	3.5		104	7.3	
106	6.4		118	9.6	
120	9.2		168	17.5	
180	21.0		182	18.4	
194	20.5		196	18.8, 20.3*	 
204	22.7		206	21.3	
206	21.9, 22.3	 	208	21.1	
208	20.6, 20.7 21.2, 21.8, 22.0	     			
210	20.7		218	24.2	
220	21.4, 22.8	 	222	20.5, 22.1	 
306	41.1		312	29.2	
312	28.2, 30.9	 			

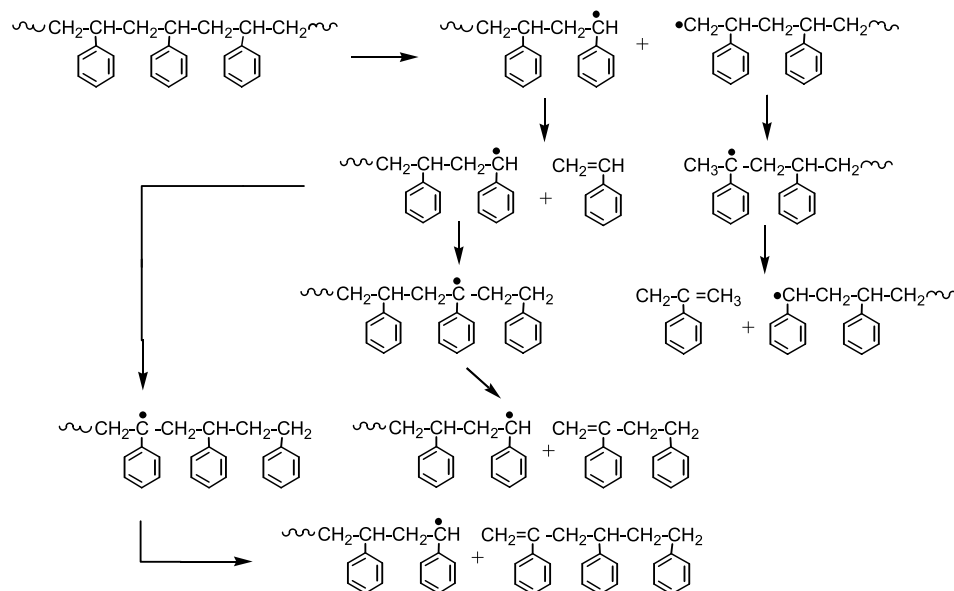
*The structure confirmed by co-injection.

head-to-head structures as well as the same evolved products as virgin PS are assigned through co-injection and/or the analysis of mass fragmentation pattern. The head-to-head structures are likely produced via radical recombination reactions followed by extensive random chain scissions, as shown in Schemes 2 and 3.

In the case of the PS nanocomposite, due to the barrier effect of the clay layers, the radicals which were produced through chain scission have more opportunity to undergo radical transfer and recombination reactions. Scheme 2 shows a possible pathway for the radical recombination reactions. Through random chain scission and radical transfer, it is thought that four radicals, denoted as A, B, C and D in Scheme 2, may be produced. Considering the

abundance and stability of radicals, A, C and D are thought to be the abundant radicals in the degradation of polystyrene nanocomposites. If these radicals undergo recombination reactions, the recombined compounds contain head-to-head structures, as shown in Scheme 2.

Due to the barrier effect of well-dispersed clay layers, some radicals and recombined molecules are trapped between the clay layers and the surrounding temperature keeps increasing during the TGA run. This provides a superheated environment in the interior part of the nanocomposite, so molecules can undergo extensive random chain scission at any methylene linkages followed by β -scission, disproportionation or hydrogen abstraction, evolving various structures, as shown in Schemes 1 and 3.



If β -scission occurs, the evolved products contain unsaturation in every molecule. Disproportionation produces molecules that exhibit both unsaturation and saturation. Hydrogen abstraction, presumably from the condensed phase, causes the production of more saturated structures. It appears that all these reactions occur in the presence of clay. For instance, there are six distinct GC peaks with an m/z 208; the 21.1 min retention time peak corresponds to styrene dimer that is produced by β -scission, and the other structures correspond to isomers such as head-to-head structures etc. that are produced via Schemes 2 and 3. The α -methyl substituted structures, such as m/z 210 (20.7 min), m/z 222 (20.5 and 22.2 min) etc., can be produced through

hydrogen abstraction or disproportionation. These support the new band at 2970 cm^{-1} due to β -carbon-hydrogen stretching mode in the presence of clay, as shown in Fig. 5.

The structures of m/z 204 (22.7 min), 218 (24.2 min) and 306 (41.3 min) include a carbon–carbon triple bond in the structure, as shown in Table 1. The structures of m/z 204 and m/z 306 were confirmed by the co-injection method with authentic compounds, which were synthesized using phenyl acetylene and Wilkinson's catalyst [27]. The presence of the carbon–carbon triple bond implies that hydrogen abstraction has occurred in the presence of clay.

It is notable that the relative intensity of 1,3 diphenylpropane (20.3 min) is increased as the clay content

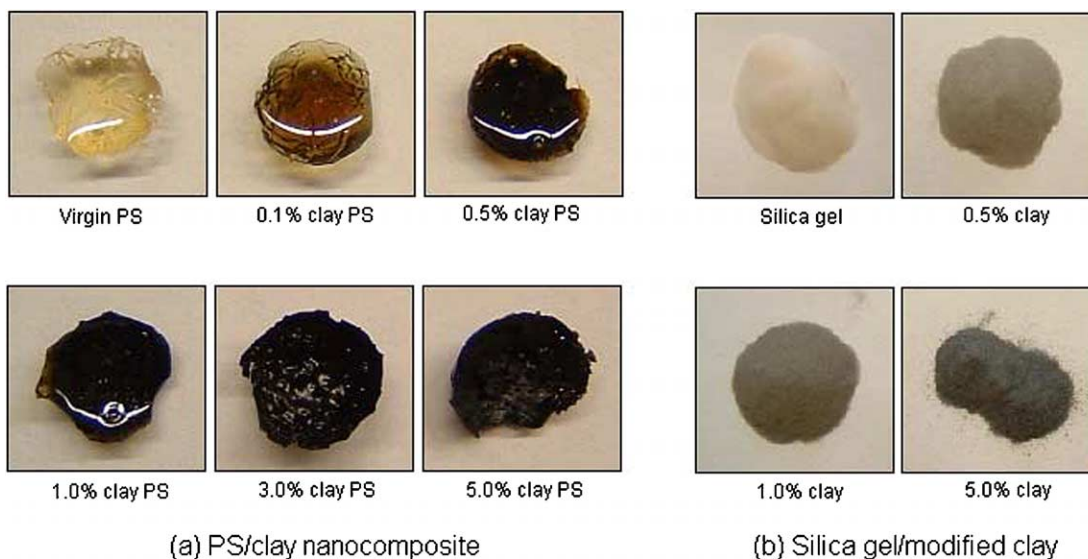
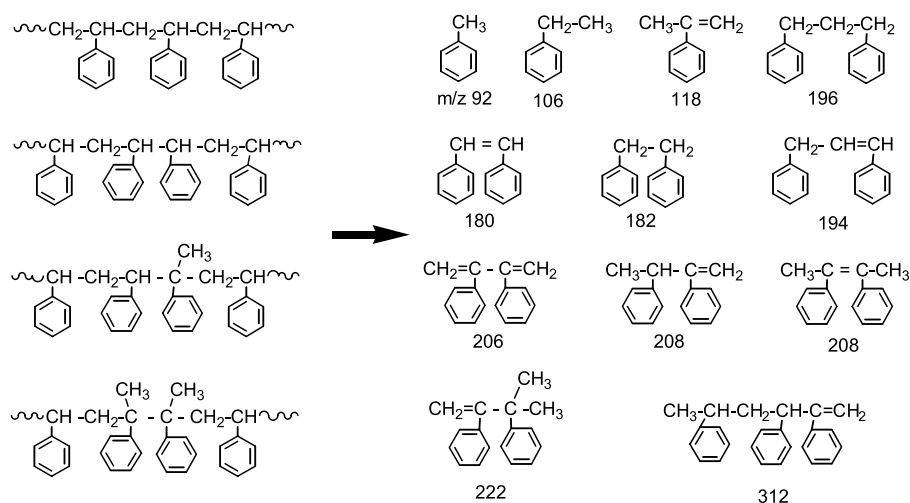
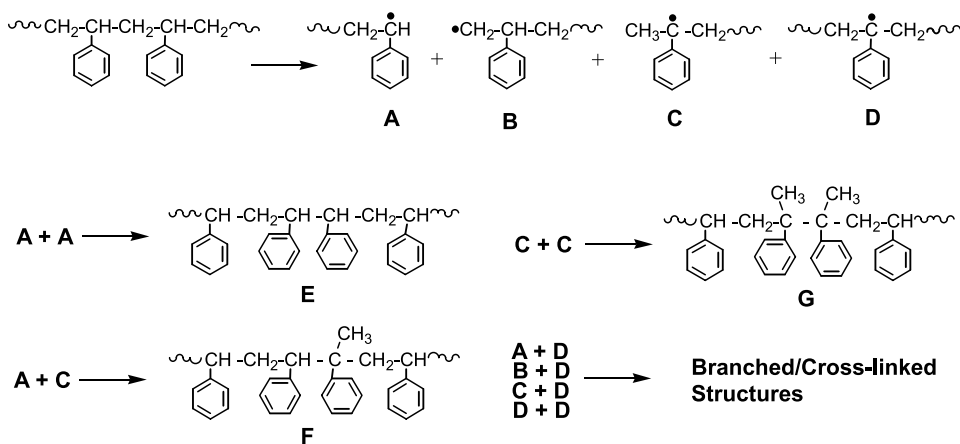


Fig. 8. (a) Residues of PS and PS nanocomposites after 40% mass loss. (b) Residues of silica gel/clay mixtures experienced the same thermal history as nanocomposites.



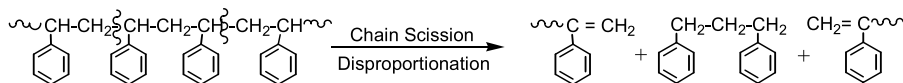
increases, as can be seen in Fig. 5. It is likely that 1,3-diphenylpropane is mainly produced through disproportionation due to the effect of the clay layers (Scheme 4). The strong intensity of 1, 3-diphenylpropane suggests that probability of disproportionation also increases in the presence of clay.

In general, inter-molecular reactions, such as hydrogen abstraction and radical recombination, become significant in the presence of clay. Due to the presence of the clay, the evolution of the degraded products from polystyrene is delayed and the products remain in the condensed phase for a longer time. Thus, the degraded products have more opportunity to undergo radical recombination reactions. At

the same time, extensive chain scission occurs, followed by β -scission (depolymerization), hydrogen abstraction and disproportionation, producing various alkyl or alkenyl phenyl structures.

3.3. Analysis of solid residue samples after 40% mass loss

In order to analyze the changes in the condensed phase during degradation, the residues after 40% mass loss were collected as a function of clay content. The color of the residues becomes darker and the luster of the residue surface is reduced with the clay content, as shown in Fig. 8. As a control, the same experiment was performed, using the



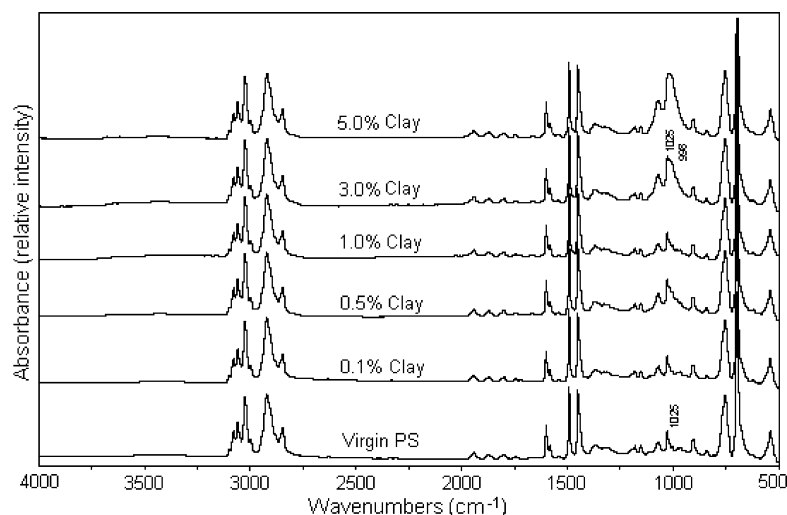


Fig. 9. FTIR of the residues at 40% mass loss for virgin polystyrene and polystyrene nanocomposites.

mixture of silica gel and modified clay, to see the color change contribution of organically-modified clay. The organic portion of the modified clay undergoes degradation and contributes to the color change to some extent, however, the color of the nanocomposite is much darker than that of the control, which implies some chemistry, such as cross-linking, conjugated double bond formation or carbonization, in the presence of clay.

To determine if cross-linking is the reason for the color change, the viscosity for the soluble portions of each formulation was measured. The portions insoluble in toluene are 2–4%, irrespective of formulation. The viscosity decreases as the clay content increases, which implies that the cross-linking may not be the important factor for the color change of PS nanocomposite. It is assumed that the cross-linked structures would dissolve and have a higher molecular weight and, hence, a higher viscosity. This viscosity trend supports the idea that extensive random chain scission has occurred in the presence of clay.

FTIR spectra were obtained for all residues and no significant change was observed, except the band at 1020 cm^{-1} , which represents silicon–oxygen stretching of clay, as shown in Fig. 9. There is no significant change in terms of carbon–carbon double bonds that are not conjugated with another unsaturated aliphatic chain. The FTIR spectra of the residues of nanocomposite at 40% mass loss are similar to those of virgin polystyrene.

The residues at 40% mass loss were extracted by solvent extraction (toluene/methanol = 1/3 v/v) and GC/MS was performed on the extracted samples and the GC traces are shown in Fig. 10. The chemical components are not different from those of the evolved products, implying that the chemical composition of the residue is the same as that of evolved products. In this case, however, the relative intensities of small molecules, such as the compounds having one benzene ring, are decreased because these are

easily evolved. As in the results of the evolved products, more components are detected with increased clay content.

The m/z 204, 218 and 306 containing carbon–carbon triple bond in one end of the structures are conjugated to carbon double bond and the assigned structures for the m/z 206 also contain conjugated double bond, as shown in Table 1. Considering these structures, it is thought that this conjugated double bond formation may contribute to the dark color of the residues of the nanocomposites and be an intermediate stage on the way to carbonization.

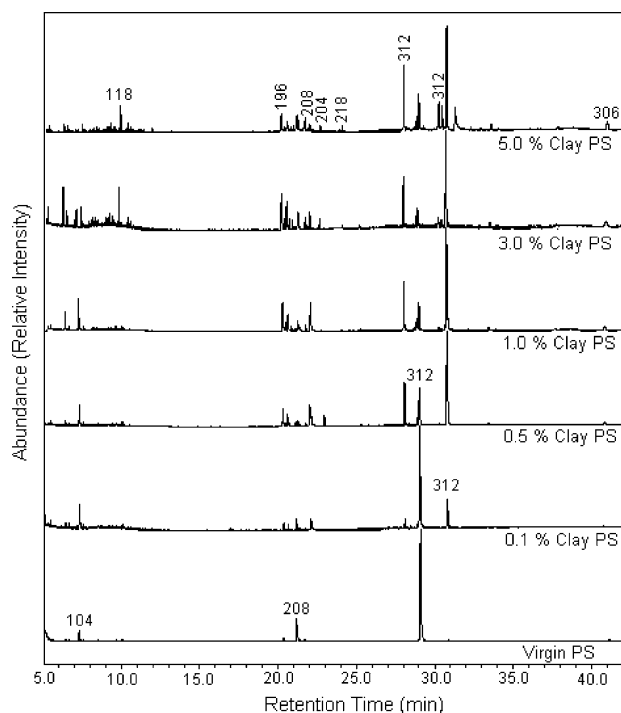


Fig. 10. GC traces of the extracted low molecular weight samples from the residues of virgin polystyrene and polystyrene nanocomposites. The inset numbers denote the m/z of the corresponding peak.

In the FTIR study, there is no significant change in the double bonds that were conjugated not to other unsaturated aliphatic chain but to the benzene ring. Since aliphatic conjugated double bonds do not have α -hydrogen, they exhibit carbon double bond stretching around 1600 cm^{-1} , which is overlapped with the benzene ring stretching, it is not possible to characterize conjugated double bonds using FTIR or even ^1H NMR. In the GC/MS study, some conjugated double bonds were observed with low intensity, and these conjugated double-bonds may be the cause of the color change.

4. Conclusion

The evolved products and residues of polystyrene and polystyrene nanocomposites were studied as a function of clay content, using TGA/FTIR and GC/MS. In the case of virgin polystyrene, the degradation produces mainly monomer, dimer and trimer through chain scission followed by β -scission (depolymerization). Since the clay layers in the nanocomposite act as a barrier to heat and mass transfer, the degradation pathway of polystyrene has been changed. In the presence of clay, additional products are evolved through radical recombination reactions and extensive random scission followed by β -scission, disproportionation and hydrogen abstraction. These reactions become significant at higher concentration of clay because the degrading polymer is retained by the clay layers, permitting further reaction. Polystyrene gives a very large reduction in the peak heat release rate; it is felt that the radical recombination reactions, which occur because of the presence of the clay, cause the retention of the degradation products for a longer period of time thus spreading out the degradation in time and reducing the peak value.

References

[1] Alexandre M, Dubois P. *Mater Sci Eng* 2000;R28:1–63.

- [2] Kojima Y, Usuki A, Kawasumi M, Okada A, Fukushima Y, Kurauchi T, et al. *J Polym Sci, Part A: Polym Chem* 1993;31:983–6.
- [3] Zhu J, Morgan AB, Lamelas FJ, Wilkie CA. *Chem Mater* 2001;13:3774–80.
- [4] Bourbigot S, Gilman JW, Wilkie CA. *Polym Degrad Stab* 2004;84:483–92.
- [5] Wilkie CA. *Recent Adv Flame Retardancy Polym Mater* 2000;11:55–7.
- [6] Zhu J, Start P, Mauritz KA, Wilkie CA. *J Polym Sci, Part A: Polym Chem* 2002;40:1498–503.
- [7] Gilman JW, Jackson CL, Morgan AB, Harris R, Manias E, Giannelis EP, et al. *Chem Mater* 2000;12:1866–73.
- [8] Zhu J, Uhl FM, Morgan AB, Wilkie CA. *Chem Mater* 2001;13:4649–54.
- [9] Wang J, Du J, Zhu J, Wilkie CA. *Polym Degrad Stab* 2002;77:249–52.
- [10] Du J, Zhu J, Wilkie CA, Wang J. *Polym Degrad Stab* 2002;77:377–81.
- [11] Du J, Wang J, Su S, Wilkie CA. *Polym Degrad Stab* 2004;83:29–34.
- [12] Du J, Wang D, Wilkie CA, Wang J. *Polym Degrad Stab* 2002;77:249–52.
- [13] Su S, Wilkie CA. *Polym Degrad Stab* 2004;83:347–62.
- [14] Kuroki T, Honda T, Sekiguchi Y, Ogawa T, Sawaguchi T, Ikemura T. *Nippon Kagaku Kaishi* 1977;894–901.
- [15] Sousa Pessoa de Amorim MT, Bouter C, Vermande P, Veron J. *J Anal Appl Pyrolysis* 1981;3:19–34.
- [16] Krauze M, Trzeszczynski J, Dzieciol M. *Polimery (Warsaw, Poland)* 2003;48:701–8.
- [17] Schroeder UKO, Ebert KH, Hamielec AW. *Makromol Chem* 1984;185:991–1001.
- [18] McNeill IC, Zulfiqar M, Kousar T. *Polym Degrad Stab* 1990;28:131–51.
- [19] Guyot A. *Polym Degrad Stab* 1986;15:219–35.
- [20] McNeill IC, Stevenson WTK. *Polym Degrad Stab* 1985;10:247.
- [21] Guaita M, Chiantore O, Costa L. *Polym Degrad Stab* 1985;12:315.
- [22] Wang D, Zhu J, Yao Q, Wilkie CA. *Chem Mater* 2002;14:3837–43.
- [23] Doh GD, Cho I. *Polym Bull* 1998;41:511–8.
- [24] Gilman JW, Kashiwagi T, Nyden M, Brown JET, Jackson CL, Lomakin S, et al. In: Al-Maliaka S, Golovoy A, Wilkie CA, editors. *Chemistry and technology of polymer additives*. London: Blackwell Scientific; 1998. p. 249–65.
- [25] Zhu J, Start P, Mauritz KA, Wilkie CA. *Polym Degrad Stab* 2002;77:253–8.
- [26] Socrates G. *Infrared and raman characteristic group frequencies*. New York: Wiley; 2001. Chapters 2 and 3.
- [27] Oshita J, Furumori K, Matsuguchi A, Ishigawa M. *J Org Chem* 1990;55:3277–80.